Journal of Catalysis **188,** 261–269 (1999)
Article ID jcat.1999.2662, available online at http://www.idealibrary.com on IDEAL®

EPR and Catalytic Investigation of Cu(Salen) Complexes Encapsulated in Zeolites

S. Deshpande, D. Srinivas, and P. Ratnasamy[1]

National Chemical Laboratory, Pune 411 008, India

Received April 12, 1999; revised August 4, 1999; accepted August 11, 1999

Zeolite-Y-encapsulated Cu(salen) and Cu(5-Cl-salen) complexes, where salen is *N*,*N*′-ethylenebis(salicylidenaminato), have been synthesized and characterized by various physicochemical techniques. "Neat" complexes showed broad EPR spectra corresponding to nearest neighbor spin–spin interactions whereas the zeolite-encapsulated metal complexes showed well-resolved metal hyperfine features similar to spectra in dilute frozen solutions indicating the encapsulation of monomeric salen complexes in zeolite cavities. Molecules adsorbed on the external surface exhibit spectra similar to "neat" complexes. The spectra arise from an unpaired electron occupying a "formal" 3$d_{x^2-y^2}$ orbital. Calculated ground-state molecular orbital coefficients suggest an increase in the in-plane covalency of the Cu–ligand bond and depletion of electron density at copper on encapsulation thereby facilitating the attack of incoming nucleophiles like *tert*-butyl hydroperoxide anion at the copper atom. In a comparitive study of the catalytic activity of the "neat" and zeolite-encapsulated Cu(salen) complexes, the activity for the decomposition of H_2O_2, *tert*-butyl hydroperoxide as well as the oxidation of phenol and *para*-xylene increased on encapsulation. The observed changes in the molecular and electronic structure of the complexes on encapsulation are, perhaps, responsible for the enhancement in catalytic activity. © 1999 Academic Press

Key Words: **copper salen; selective catalytic oxidation; EPR spectra of copper complexes; encapsulation in zeolite; electronic structure of encapsulated complexes.**

INTRODUCTION

Transition metal salen complexes, where salen is *N*,*N*′-ethylenebis(salicylidenaminato), are functional mimics of metalloproteins in dioxygen binding and oxidation of olefins and aromatic compounds using hydrogen peroxide, iodosylbenzene, NaOCl, etc. (1–3). The Schiff base salen complexes are conformationally flexible and adopt a variety of geometries, viz., planar, umbrella-type, and stepped conformations, to generate various active site environments for the different oxidation reactions (4, 5). This flexibility, similar to that observed in metalloproteins, is a key factor for the biomimetic activity of these molecules.

Encapsulation of these salen complexes in the supercages of zeolites X and Y and mesoporous materials leads to solid catalysts which, in addition to possessing the engineering advantages of heterogeneous catalysts like ruggedness, easy catalyst separation, etc., also share many advantageous features of homogeneous catalysts like a well-defined unique structure which can be elucidated and correlated with catalytic activity. But unlike their homogeneous counterparts, they are not easily deactivated by dimer/polymer formation. We have recently reported the catalytic activity of zeolite-encapsulated complexes of copper like copper acetate monohydrate (6), copper phthalocyanines (7), and copper salens (8–14) for the selective oxidation of methane, propane, aliphatic and aromatic hydrocarbons, hydroxylation of phenols to diphenols, epoxidation of olefins, oxyhalogenation of aromatic compounds, and the decomposition of H_2O_2 (to H_2O and O_2) and *tert*-butyl hydroperoxide. We had found that, in all cases, the intrinsic activity of the copper complexes is enhanced significantly on encapsulation in zeolites. In an attempt to understand this enhancement in catalytic activity (and in some cases catalytic selectivity), we have, now, undertaken an investigation of the structural changes undergone by the copper complexes when encapsulated in the cavities of zeolites using various physicochemical techniques. The present paper reports an EPR investigation of the changes in the molecular structure of copper salen and 5-chloro copper salen on encapsulation in zeolite Y. Corresponding changes in oxidation activity are also reported.

The EPR signals of neat Cu(II) complexes in the polycrystalline state are usually broadened due to dipolar and spin–spin exchange interactions. Consequently, structural information from the hyperfine and superhyperfine coupling interactions between the unpaired electron and copper and surrounding magnetic nuclei, respectively, is lost and the *g* values are not the molecular values. Encapsulation of complexes in the supercages of zeolites results in isolation and dilution of the paramagnetic complex in a diamagnetic aluminosilicate matrix and, hence, is expected

[1] To whom correspondence should be addressed. E-mail: prs@ems.ncl.res.in. Fax: (91)-20-5893355/5894761.

0021-9517/99 $30.00

to yield resolved signals. Moreover, depending upon the size of the encapsulated molecule, the EPR spectra, in ideal cases, might also throw light on the mobility of the molecule and its preferred molecular conformations in the zeolite cavities. The latter information is crucial in deriving structure–activity correlations in such "zeozyme" systems. To our knowledge, this is the first EPR study of encapsulated Schiff base Cu(II) complexes in zeolites.

EXPERIMENTAL

Materials and Synthesis of "Neat" and Zeolite-Encapsulated Copper Salens 1–4

The Schiff base ligands, *N*,*N*′-ethylenebis(salicylideamine) (salenH_2) and *N*,*N*′-ethylenebis(5-chlorosalicylideamine) (5-Cl-salenH_2), were prepared according to procedures described in the literature (4). The copper complexes, Cu(salen) **1** and Cu(5-Cl-salen) **2**, were synthesized by mixing equimolar ethanolic solutions of $Cu(CH_3COO)_2 \cdot 4H_2O$ and the corresponding Schiff base ligand. The solutions were gently heated for 1 h while stirring and allowed to cool. The complexes thus obtained were recrystallized from chloroform and their purity was checked by elemental analysis, FTIR, and UV–vis spectroscopic techniques.

We followed the "flexible ligand" method (10) to obtain samples of zeolite-Y-encapsulated Cu(salen) and Cu(5-Cl-salen) complexes (samples **3** and **4**, respectively). In this procedure, the corresponding Schiff base ligand (salenH_2 or 5-Cl-salenH_2) was taken in a round bottom flask immersed in an oil bath of temperature 428 K. Copper(II) exchanged Na–Y (ligand : Cu–Y = 3 : 1) was added to this and the reaction was continued for 24 h. The green solid formed was separated and Soxhlet-extracted with $CHCl_3$ for about 5 days until the extract was colorless. Physicochemical characterizations of the materials were carried out as reported in our earlier publications (7–14). The amount of copper loading was estimated to be 1.93 wt%.

Methods: EPR Spectroscopy

Electron paramagnetic resonance spectra were recorded on a Bruker EMX X-band spectrometer with 100 kHz field modulation. Measurements were performed on powder samples at 298 and 77 K. DPPH was used as a field marker ($g = 2.0036$). Experiments at 77 K were carried out using a quartz inserting Dewar. The spin Hamiltonian parameters were determined by simulating the spectra using a Bruker Simfonia software package. The diffuse reflectance UV–visible spectra were measured using a UV-101 PC Shimadzu spectrophotometer.

Catalytic Activity

Decomposition of H_2O_2. "Neat" or encapsulated complex (0.025 g) was stirred in 5.5 g H_2O_2 (30% aqueous) solution at 298 K for 1 h. After filtration of the catalyst, the product was diluted with water to 250 ml. To 10 ml of this solution, 20 ml dilute sulfuric acid (1 : 20) and 20 ml water were added. The solution was then titrated against standard $KMnO_4$.

Decomposition of tert-butyl hydroperoxide (TBHP). Neat or encapsulated complex (0.025 g) was stirred in 5 g of TBHP at 298 K for 1 h. At the end of the reaction time the extent of decomposition of TBHP was estimated by standard iodimetry.

Oxidation of phenol. Phenol (4.7 g) and catalyst (0.05 g) were taken in a glass reactor. Drop by drop, 1.13 g of 30% H_2O_2 was added. The reaction was carried out for 1 h at 353 K. At the end of 1 h, the reaction mixture was cooled to room temperature and the products were analyzed by a gas chromatograph (Hewlett–Packard 5880) equipped with a SE 30 column. The identity of the products was further confirmed by GC-MS (Shimadzu GC-MS QP 5000).

Oxidation of para-xylene. The oxidation of *para*-xylene was carried out in an Parr autoclave of 300 ml volume. In a typical experiment, 30 g of *para*-xylene, 0.5 g of solid catalyst, and 0.5 g of *tert*-butyl hydroperoxide were taken in an autoclave and pressurized with air to 33 bar. The reaction mixture was stirred continuously at 403 K for 18 h. After the completion of the reaction, the autoclave was cooled and the catalyst was removed by hot filtration. The resultant filtrate was cooled to crystallize *para*-toluic acid which was removed by filtration. The final filtrate contains *p*-toluyl aldehyde, *p*-tolyl alcohol, 4-carboxybenzyl alcohol, 4-carboxy benzaldehyde, and unreacted *p*-xylene. There was only a trace of other acids (like terephthalic acid) in the solid products. The acids formed were esterified and analyzed as methyl esters by the procedure given below: 300 μl of the sample was taken in a glass vial. Two milliliters of 14% boron trifluoride (BF_3) in methanol was added to the glass vial which was stoppered with a Teflon-lined stopper and heated for 1 h at 353 K. The sample was cooled to room temperature and 2 ml of Milli-Q reagent water was added with mild shaking. HPLC grade dichloromethane (2 ml) (S.D. Fine Chemicals, India) was added before the GC analysis. The identity of the products was further confirmed by GC-MS (Shimadzu QCMC-QP 2000A). The liquid products of the oxidation reaction were analyzed in a gas chromatograph (Shimadzu GC 14B) equipped with a SE-32 column and a flame ionization detector.

RESULTS AND DISCUSSION

EPR Spectroscopy

EPR spectra for the "neat" complexes (**1** and **2**) as polycrystals are characterized by an axial *g* tensor. Hyperfine features due to copper ($S = 1/2$ and $I = 3/2$) could not be resolved even at 77 K due to intermolecular spin–spin

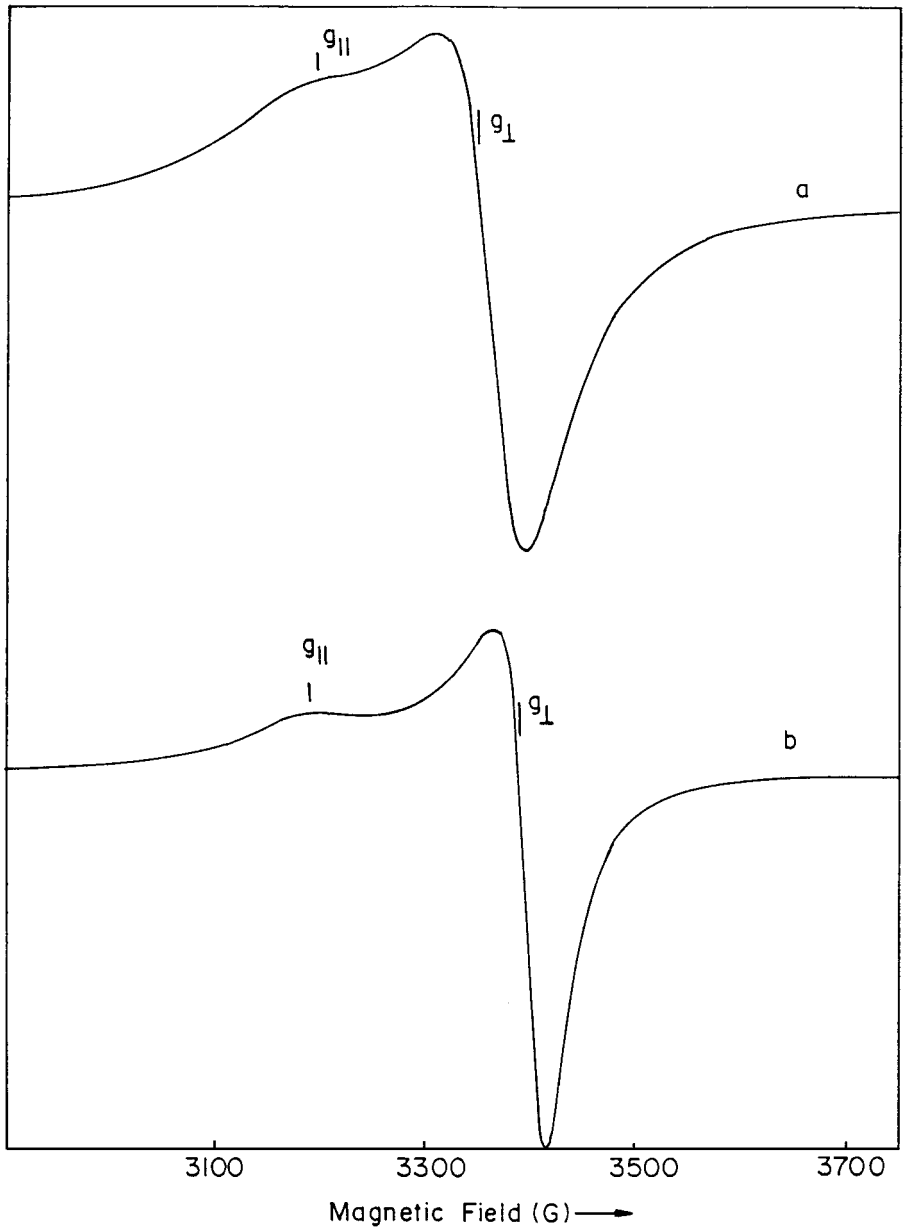

FIG. 1. X-band EPR spectra of polycrystalline samples of "neat" Cu(Salen) (a) and Cu(5-Cl-Salen) (b).

exchange interactions. Typical spectra at 298 K are shown in Fig. 1. The spectral features are broader for Cu(salen) than for Cu(5-Cl-salen) consistent with the dimeric molecular association in the former case in solid state, while the latter is monomeric (4).

The spectra for the zeolite-encapsulated metal complexes **3** and **4** are shown in Figs. 2 and 3, respectively, and could be interpreted using the following spin Hamiltonian formalism for axial symmetry (15).

$$\mathcal{H} = \beta_e[g_\parallel H_z S_z + g_\perp (H_x S_x + H_y S_y)] + A_\parallel I_z S_z + A_\perp (S_x I_x + S_y I_y) \quad [1]$$

Here, β_e is the Bohr magneton and the rest of the terms carry their usual meaning. Hyperfine features due to copper could be resolved in the parallel region for both the encapsulated complexes (**3** and **4**) while only Cu(salen)-Y (**3**) shows partial resolution in the perpendicular region (Figs. 2c and 3c). The spectra for frozen solutions of "neat" Cu(5-*X*-salen) **1** and **2** (2×10^{-3} M) are shown in Figs. 2a and 2b and 3a and 3b, respectively. Hyperfine coupling due to copper is resolved in both the parallel and perpendicular regions. Further dilutions of the sample did not improve the resolution any more and indicate that the molecules are isolated and no interaction is present between the individual molecule of the Cu(5-*X*-salen) complexes in such a

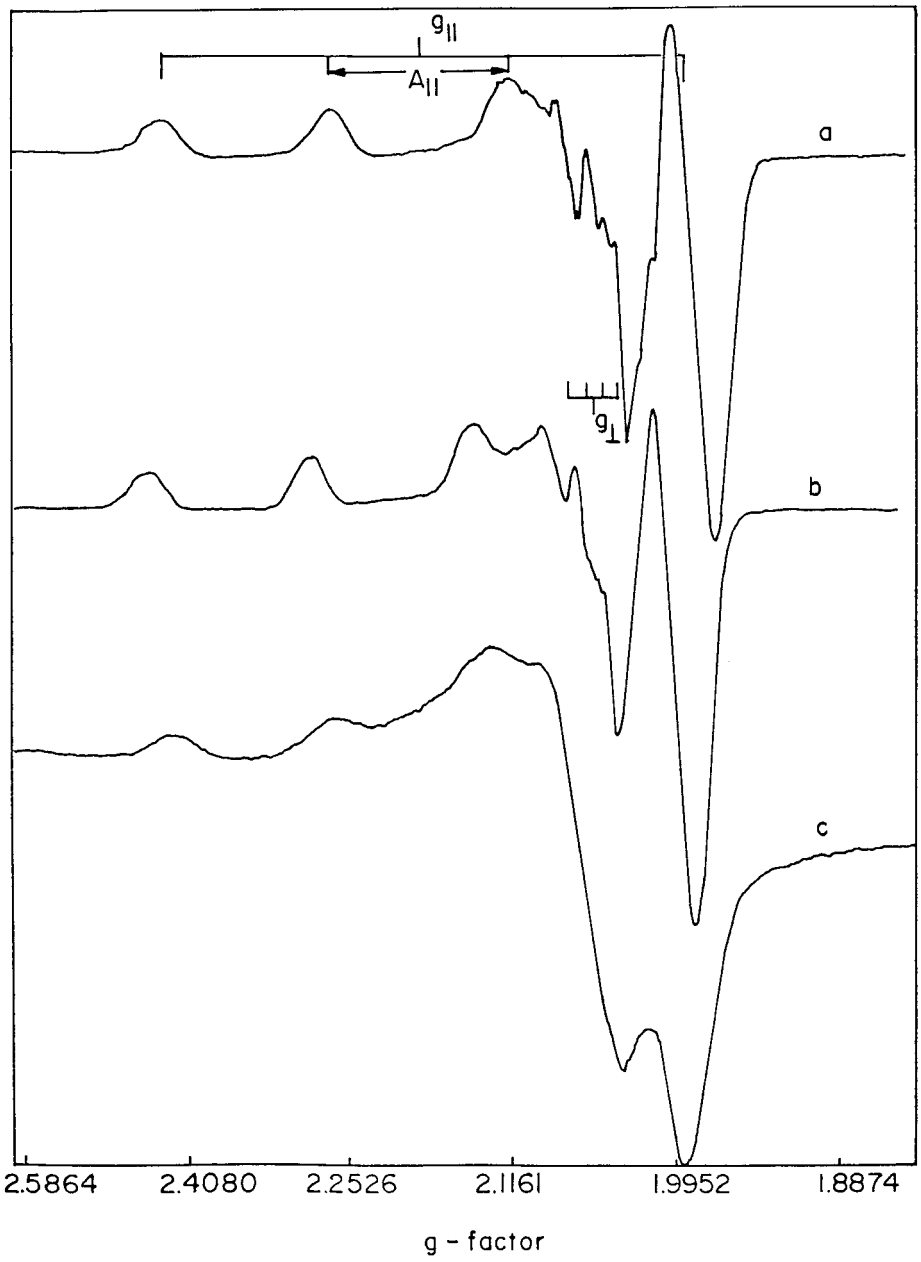

FIG. 2. EPR spectra of Cu(Salen) as (a) frozen $CHCl_3/CH_3CN$ (3 : 1) solution (77 K), (b) frozen DMF solution (77 K), and (c) zeolite-encapsulated complex.

diluted solutions. Interestingly, the spectra of encapsulated complexes **3** and **4** are almost similar to that of frozen solutions (Figs. 2 and 3) and, hence, indicate the encapsulation of individual molecules of Cu(5-*X*-salen), $X = H$ and Cl, in the supercages of Na–Y. The intermolecular interactions are avoided due to isolation in the zeolite cavities and thereby resolved metal hyperfine features are observed even in the solid state in encapsulated metal complexes. Spectra for the surface adsorbed species (not shown) resembled that of neat samples in solid state. EPR spectroscopy can thus be used as an analytical tool to distinguish transition metal complexes encapsulated in zeolites. From a comparitive spectral intensity, obtained by double integration of the first derivative EPR spectrum, the amounts of Cu(5-*X*-salen) encapsulated in NaY are estimated. One molecule of the copper complex is encapsulated in every seven supercages of Na–Y for Cu(salen) and in every nine supercages of Na–Y for Cu(5-Cl-salen). The spin Hamiltonian parameters for the encapsulated and "neat" complexes are listed in Table 1. The *g* values for the zeolite-encapsulated complexes are similar to that of the "neat" complexes. The Cu hyperfine features are, however, resolved only in the

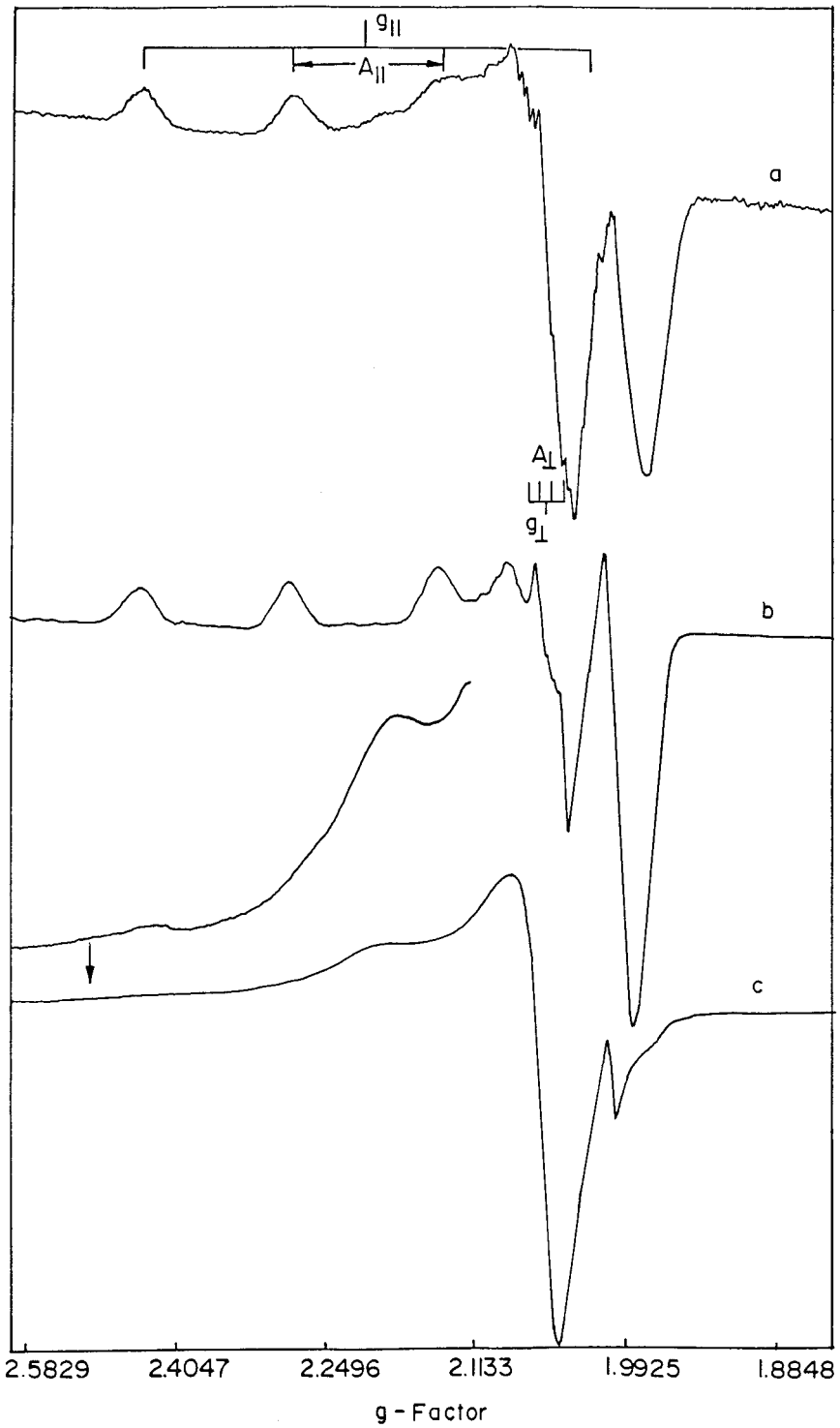

FIG. 3. EPR spectra for Cu(5-Cl-Salen) as (a) frozen $CHCl_3/CH_3CN$ (3:1) solution (77 K), (b) frozen DMF solution (77 K), and (c) zeolite-encapsulated complex.

former case. The EPR parameters of the neat complexes, especially $g_\parallel$ and $A_\parallel$, vary with the solvents used. Larger $g_\parallel$ and lower $A_\parallel$ values, observed in the case of frozen DMF solutions, suggest the coordination of solvent DMF as an axial ligand and more delocalization of charge onto the ligand orbitals due to formation of a square pyramidal structure (16).

The EPR spectra of the encapsulated complexes (Figs. 2c and 3c) are somewhat broader than those for frozen

TABLE 1

EPR Data for Substituted Cu(Salen) Complexes as "Neat" and Encapsulated in Zeolite Y

Complex	State	Color	Temp. (K)	$g_{\|\|}$	$g_\perp$	$A_{\|\|}$ (G)	$A_\perp$ (G)
Cu(Salen)	Neat polycryst.	Green	298	2.199	2.072	NR[a]	NR
	Encapsulated	Cream	298	2.198	2.068	210	23
	$CHCl_3$/CH_3CN (3:1)	Bluish violet	77	2.195	2.065	206	30
	DMF	Blue	77	2.212	2.050	195	30
Cu(5-Cl-Salen)	Neat polycryst.	Brown	298	2.195	2.052	NR	NR
	Encapsulated	Cream	298	2.194	2.060	202	25
	$CHCl_3$/CH_3CN (3:1)	Greenish blue	77	2.214	2.053	200	23
	DMF	Blue	77	2.218	2.048	191	29

[a] NR, not resolved.

solutions suggesting that the complexes located in the supercages could be present in more than one geometrical conformation. The overlap of the spectra due to individual conformational geometries can account for the broader spectral lines. Perhaps line narrowing and resolution of copper sites could be achieved at *Q*-band frequency.

Ground-State Wave Function and Bonding Parameters

The molecular g values for the frozen solutions and zeolite-encapsulated metal complexes (Table 1) with $g_{\|} > g_\perp$ indicate that the unpaired electron occupies a "formal" $d_{x^2-y^2}$ orbital. The ground-state wave function and bonding parameters were evaluated using the ligand field approach originally developed by Maki and McGarvey (17) and later modified by Kivelson and Neiman (18) for lower D_{2h} symmetry. From the differences between the N and O atoms, the molecular symmetry at the site of copper could be described as C_{2v}. However, the axial EPR spectrum, instead of a rhombic spectrum usually expected for this low symmetry, suggests a higher electronic symmetry, close to that of a square planar complex. Hence the approach adopted by Maki and McGarvey (17) and Kivelson and Neiman (18) could be applied for the present complexes. The molecules in the encapsulated state may be present in more than one molecular conformation. However, all these conformations possess electronic symmetry close to C_{4v}. For the square planar complex the following anti-bonding molecular orbitals for the "hole" configuration, labeled according to the symmetry, can be formed from the metal 3*d* orbitals and the ligand (N, O) 2*s* and 2*p* orbitals. The four ligands are placed on the $\pm x$ and $\pm y$ axes. The positive sign applies to the ligand atoms on the positive x and y axes and the negative sign to those on the negative x and y axes of the square planar geometry.

$$\begin{aligned}
\psi(b_{1g}) &= \alpha d_{x^2-y^2} - \alpha'(-\sigma_{x^1} + \sigma_{y^2} + \sigma_{x^3} - \sigma_{y^4})/2 \\
\psi(b_{2g}) &= \beta d_{xy} - \beta'(p_{y^1} + p_{x^2} - p_{y^3} - p_{x^4})/2 \\
\psi(a_{1g}) &= \alpha_1 d_{3z^2-r^2} - \alpha_1'(\sigma_{x^1} + \sigma_{y^2} - \sigma_{x^3} - \sigma_{y^4})/2 \\
\psi(E_g) &= \begin{matrix} \delta d_{xz} - \delta'(p_{z^1} - p_{z^3})/\sqrt{2} \\ \delta d_{yz} - \delta'(p_{z^2} - p_{z^4})/\sqrt{2}, \end{matrix}
\end{aligned} \qquad [2]$$

where $\sigma^{(i)} = np^{(i)} -/+ (1-n^2)^{1/2}s^{(i)}$ and $0 \le n \le 1$. α and β are the metal d orbital coefficients for the MOs b_{1g} and b_{2g} representing the in-plane σ and π bonding, respectively, while δ is the coefficient for the MO e_g representing the out-of-plane π bonding. α' is the coefficient for the ligand orbitals forming b_{1g} molecular orbital and is related by the normalization expression as

$$\alpha^2 + \alpha'^2 - 2\alpha\alpha' S = 1. \qquad [3]$$

Here S is the overlap integral between the metal $d_{x^2-y^2}$ and ligand σ orbitals. The expressions for the g and hyperfine coupling constants (A_{Cu}) in terms of MO coefficients can be derived by solving the above Hamiltonian (Eq. [1]) and employing the wave functions given by Eq. [2]

$$\begin{aligned}
g_{\|} &= 2.0023 - (8\lambda\alpha\beta/\Delta E_{xy})[\alpha\beta - \alpha'\beta S \\
&\quad - \alpha'(1-\beta^2)^{1/2}T(n)/2] \\
g_\perp &= 2.0023 - (2\lambda\alpha\delta/\Delta E_{xz,yz})[\alpha\delta - \alpha'\delta S \\
&\quad - \alpha'(1-\delta^2)^{1/2}T(n)/\sqrt{2} \\
A_{\|} &= P\{-\alpha^2(4/7 + k_0) + (g_{\|} - 2) + (3/7)(g_\perp - 2) \\
&\quad - (8\lambda\alpha\beta/\Delta E_{xy})[\alpha'\beta S + \alpha'(1-\beta^2)^{1/2}T(n)/2] \\
&\quad - (6/7)(\lambda\alpha\delta/\Delta E_{xz,yz})[\alpha'\delta S + \alpha'(1-\delta^2)^{1/2}T(n)/\sqrt{2}]\} \\
A_\perp &= P\{\alpha^2(2/7 - k_0) + (11/14)(g_\perp - 2) - (22/14) \\
&\quad \times (\lambda\alpha\delta/\Delta E_{xz,yz})[\alpha'\delta S + \alpha'(1-\delta^2)^{1/2}T(n)/\sqrt{2}]\},
\end{aligned} \qquad [4]$$

where $T(n) = n - (1-n^2)^{1/2}R^8(Z_pZ_s)^{5/2}(Z_s - Z_p)/(Z_s + Z_p)^5 a_0$ and $P = 2\beta\beta_N g_N \langle d_{x^2-y^2}|r^{-3}|d_{x^2-y^2}\rangle$ and λ is the spin-orbital coupling constant and is -828 cm^{-1} for the free Cu(II) ion (19). The overlap integral S and the constant $T(n)$ were taken as 0.093 and 0.333, respectively (17, 18). The dipolar interaction term P was taken as 0.036 cm^{-1} (17, 18). The MO coefficients (α, α', β, and δ) were estimated from the experimental spin Hamiltonian parameters (Table 1) and the g and A value expressions.

UV–visible and diffused reflectance spectra (12, 13) showed a resolved excitation band for $B_{1g} \leftrightarrow A_g$ in the range 17,360–17,730 cm^{-1} while the band due to $B_{1g} \leftrightarrow E_g$ could be resolved only in a few cases. Thus, the in-plane π bonding (β) could be calculated in all the cases whereas δ was

TABLE 2

MO Coefficients in D_{4h} Symmetry and Electronic *d–d* Transition Energies for Substituted Cu(Salen) Complexes

Complex	State	MO coefficients				*d–d* transition energies (cm^{-1})	
		α^2	α'^2	β^2	δ^2	ΔE_{xy}	$\Delta E_{xy,yz}$
Cu(Salen)	Encapsulated	0.839	0.245	0.588		17,391	
	$CHCl_3/CH_3CN$	0.826	0.260	0.596		17,730	
	DMF	0.805	0.284	0.645		17,361	
Cu(5-Cl-Salen)	Encapsulated	0.811	0.278	0.588		17,391	
	$CHCl_3/CH_3CN$	0.807	0.282	0.664	0.880	17,731	24,390
	DMF	0.799	0.290	0.666	0.779	17,361	23,810

estimated only in those cases where $B_{1g} \leftrightarrow E_g$ was resolved. Table 2 presents the MO coefficients and the excitation band energies for solutions and zeolite-encapsulated complexes.

The MO coefficients (Table 2), in general, are smaller than unity indicating the covalent nature of bonding between metal and ligand orbitals. They vary in the order $\beta < \alpha \leq \delta$ suggesting that the in-plane π bonding (between $3d_{xy}$ and p_π orbitals) is more covalent than the in-plane σ bonding (between $3d_{x^2-y^2}$ and p_σ orbitals). The latter is, in turn, more covalent than the out-of-plane π bonding (between $3d_{xz/yz}$ and p_π orbitals). The MO coefficients are modified considerably on encapsulation. The coefficient α, characteristic of in-plane σ bonding, increases while β, characteristic of in-plane π bonding, decreases on encapsulation. These results highlight the structural changes in the Schiff base complexes on encapsulation. These changes are, apparently, more for Cu(salen) than for Cu(5-Cl-salen) (see Table 2). The higher in-plane covalency as indicated by a smaller α value and lower hyperfine coupling constant for Cu(5-Cl-salen) suggests a relatively larger depletion of electron density at the site of copper. Encapsulation in zeolites, hence, leads to depletion of electron density at the copper site. This depletion, in turn, will facilitate nucleophilic attack by reagents like *tert*-butyl hydroperoxide anion at the metal center. Since transition metal hydroperoxides are known oxidation catalysts, an enhancement in their rates of formation will increase the catalytic activity. The catalysis results (*vide infra*) are in good agreement with these EPR observations.

Catalytic Activity

The catalytic activity of the neat and zeolite-encapsulated copper salen and copper chloro–salen complexes in the oxidation of *para*-xylene (to mainly *para* toluic acid) and phenol (to catechol and hydroquinone) and in the decomposition of H_2O_2 (to H_2O) and TBHP (to *tert*-butanol) are shown in Table 3. Two features may be noted: (1) The catalytic activity of both the salen and chloro–salen complexes is enhanced significantly on encapsulation in zeolite Y. (2) Catalytic activity is also enhanced when chlorine is substituted for H atoms in the salen ligand. A preliminary study of the catalytic activity of zeolite-encapsulated copper salens and substituted copper salens has been reported by us earlier (9–14). We had shown (11) that copper ions leached out of the zeolite during the reaction, if any, cannot make a significant contribution to the observed catalytic activity. In fact, the significant enhancement (by orders of magnitude) in the intrinsic catalytic activity (turnover frequencies) of the zeolite-encapsulated salens (Table 3) vis-a-vis the "neat" complexes is a strong indication that it is the catalytic behavior of the isolated copper salens inside the cavities of the zeolite that is responsible for the observed enhancement in catalytic activity. The activity of the leached complexes, if any, would have been lower, similar to solutions of the "neat" complex. It should also be noted that the turnover frequencies (in Table 3) have been calculated on the basis of the total copper ions present in the solid and represent the minimum values since only a fraction of the copper ions encapsulated in the zeolite are expected

TABLE 3

Catalytic Activity of "Neat" and Zeolite-Encapsulated Substituted Cu(Salen)[a]

Catalyst	Catalytic activity			
	p-Xylene oxidation (% wt)	Phenol oxidation (% wt)	TBHP conv. (TOF, h^{-1})	H_2O_2 conv. (TOF, h^{-1})
Cu(Salen)	3.4	6.2 (21)	53	36
Cu(5-Cl-Salen)	4.6	7.7 (31)	108	64
Cu(Salen)-Y	45.1	5.4 (40)	1704	232,506
Cu(5-Cl-Salen)-Y	48.9	6.8 (88)	29,377	454,949

[a] See text for reaction conditions and product distribution. Values in parentheses refer to TOF, h^{-1} values. TOF, h^{-1} = moles of substrate converted per mole of copper (in the solid catalyst) per hour.

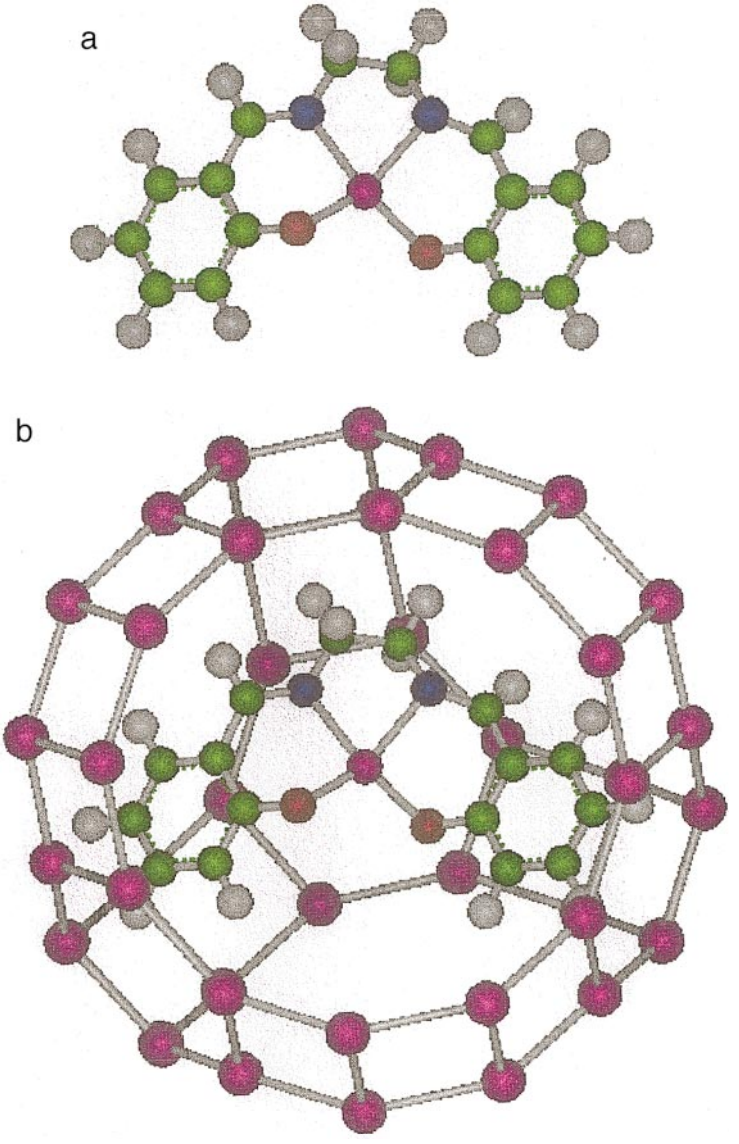

FIG. 4. The structures of "neat" Cu(Salen) dissolved in noncoordinating solvents (a) and Cu(Salen) encapsulated in zeolite Y (b).

to contribute to the observed catalytic activity due to diffusional and other constraints on those located deeper in the core of the zeolite particle. The 'true' TOF values may be significantly higher. Recalling our EPR results (see earlier) that indicate the absence of copper salens adsorbed on the external surface of the zeolite particles (such species having been carefully washed away during the preparation procedure), we may conclude that the observed enhancement in intrinsic catalytic activity is a consequence of encapsulation.

Structure–Activity Correlations

The structures of Cu(Salen) encapsulated in zeolite Y, obtained after geometry minimization, and "neat" Cu(Salen) in the dissolved liquid state are shown in Fig. 4. "Neat" Cu(Salen) in the *solid state* is dimeric and the copper complex has a tetragonally elongated square pyramidal configuration with the donor atoms, N_2O_2, forming a perfect basal plane (4). However, in the dissolved state and in noncoordinating solvents, the complex exists as a monomer with square planar geometry as shown in Fig. 4. The present EPR and geometry minimization studies indicate that in the encapsulated complex, Cu(salen) is present as monomers (as in the dissolved state) in the super cages of zeolite Y. Further, the geometry is distorted square planar as shown in Fig. 4. Cu(5-Cl-salen) possesses a distorted square planar configuration in both "neat" and encapsulated states. The higher observed catalytic activity of "neat" Cu(5-Cl-salen) (Table 3) is probably due to the depletion of electron

density at the site of copper by the electron withdrawing chlorine. Such a depletion is indicated by (i) our EPR results wherein a higher in-plane covalency and lower hyperfine coupling constants were observed for Cu(5-Cl-salen), and (ii) our earlier result (4) that the Cu(II)/Cu(I) couple appears at less negative potentials for Cu(5-Cl-salen) than for Cu(salen). Our EPR results suggest that the encapsulated complexes (or at least a significant fraction of them) are present in a distorted tetrahedral conformation. A tetrahedral distortion of the square planar complex will increase the Cu(II)/Cu(I) reduction potential leading to a further enhancement of the oxidation reaction. It may be borne in mind that while Cu(II) complexes prefer square planarity, tetrahedral symmetry is favored by Cu(I) complexes. Changes in the Cu(II)/Cu(I) reduction potentials of the copper salen complexes (brought about either by substitution of electron-withdrawing groups or encapsulation in zeolites) are, thus, responsible for their catalytic activity.

SUMMARY AND CONCLUSIONS

EPR spectroscopy has been used to provide unequivocal evidence for the encapsulation of Cu(salen) and Cu(5-Cl-salen) complexes in the supercages of zeolite Y. While the surface-adsorbed salen complexes showed spectra similar to that of "neat" complexes in the solid state (dimeric in the case of Cu(Salen)), the zeolite-encapsulated species showed well-resolved hyperfine features characteristic of isolated monomeric copper complexes in the diamagnetic zeolite matrix. The spin Hamiltonian parameters (reduced copper hyperfine coupling) and the molecular orbital coefficients for the HOMOs revealed enhanced covalency as a consequence of changes in molecular structure due to encapsulation. The enhanced catalytic activity of the zeolite-encapsulated copper salens in the oxidation of phenol/*para*-xylene and the decomposition of H_2O_2/TBHP probably arises from these changes in the molecular and electronic structure of the complexes on encapsulation in the zeolite cavities.

ACKNOWLEDGMENT

We thank Drs. Chandra R. Jacob and S. P. Varkey for the catalytic data and Mr. Suresh B. Waghmode for the help in modeling studies.

REFERENCES

1. Balkus, K. J., Jr., and Gabrielov, A. G., *J. Incl. Phenom. Mol. Recog. Chem.* **21**, 159 (1995).
2. Bowers, C., and Dutta, P. K., *J. Catal.* **122**, 271 (1990).
3. Balkus, K. J., Jr., Welch, A. A., and Gnade, B. E., *Zeolites* **10**, 722 (1990).
4. Bhadbhade, M. M., and Srinivas, D., *Inorg. Chem.* **32**, 5458 (1993).
5. Bhadbhade, M. M., and Srinivas, D., *Polyhedron* **17**, 2699 (1998).
6. Raja, R., and Ratnasamy, P., *J. Mol. Catal. A: Chem.* **100**, 93 (1995).
7. Raja, R., and Ratnasamy, P., *Appl. Catal.: General A* **158**, L7 (1997).
8. Raja, R., and Ratnasamy, P., *J. Catal.* **170**, 244 (1997).
9. Raja, R., and Ratnasamy, P., *Stud. Surf. Sci. Catal.* **101**, 181 (1996).
10. Ratnasamy, C., Murugkar, A., Padhye, S., and Pardhy, S. A., *Indian J. Chem. A* **35**, 1 (1996).
11. Jacob, C. R., Varkey, S. P., and Ratnasamy, P., *Microporous Mesoporous Mat.* **22**, 465 (1998).
12. Jacob, C. R., Varkey, S. P., and Ratnasamy P., *Appl. Catal. A: General* **168**, 353 (1998).
13. Varkey, S. P., Ratnasamy, C., and Ratnasamy, P., *J. Mol. Catal. A: Chem.* **135**, 295 (1998).
14. Jacob, C. R., Varkey, S. P., and Ratnasamy, P., *Appl. Catal. A: General* **182**, 91 (1999).
15. Wertz, J. E., and Bolton, J. R., "Electron Spin Resonance: Elementary Theory and Practical Applications," Chap. 7, pp. 131–163. McGraw-Hill, New York, 1972.
16. Hathaway, B. J., *in* "Comprehensive Coordination Chemistry" (Sir G. Wilkinson, F.R.S. Ed.), Vol. 5, Chap. 53, pp. 533–774. Pergamon Press, Oxford, 1987.
17. Maki, A. H., and McGarvey, B. R., *J. Chem. Phys.* **29**, 31 & 35 (1958).
18. Kivelson, D., and Neiman, R., *J. Chem. Phys.* **35**, 149 (1961).
19. Abragam, A., and Bleaney, B., *in* "Electron Paramagnetic Resonance of Transition Ions," Chap. 7, p. 378, Clarendon Press, Oxford, 1970.